FRONTIERS OF PHYSICS

TOPICAL REVIEW
Volume 21 / Issue 11 / 115301 / 2026

Progress of ambient-pressure superconductivity in bilayer nickelate thin films

Wenyuan Qiu, Dao-Xin Yao†

Guangdong Provincial Key Laboratory of Magnetoelectric Physics and Devices,
State Key Laboratory of Optoelectronic Materials and Technologies, School of Physics,
Sun Yat-sen University, Guangzhou 510275, China
Corresponding author. E-mail: †yaodaox@mail.sysu.edu.cn
Received March 7, 2026; accepted May 6, 2026

ABSTRACT

This review summarizes recent progress of ambient-pressure superconductivity in bilayer nickelate $La_3Ni_2O_7$ thin films, a major advancement following the discovery of high-pressure superconductivity in bulk $La_3Ni_2O_7$. First, we explain how epitaxial strain engineering enables ambient-pressure superconductivity in $La_3Ni_2O_7$ thin films, with compressive strain from substrates like $SrLaAlO_4$ stabilizing superconductivity. Next, we review experimental characterizations of related systems, with particular emphasis on ARPES measurements that have shown conflicting Fermi surface topologies. We then discuss progress in increasing the superconducting transition temperature T_c. Finally, we summarize theoretical studies of the electronic structure and pairing symmetry of $La_3Ni_2O_7$ thin films. Together, these advances establish bilayer nickelate thin films as a highly tunable and promising platform for exploring high-T_c superconductivity.

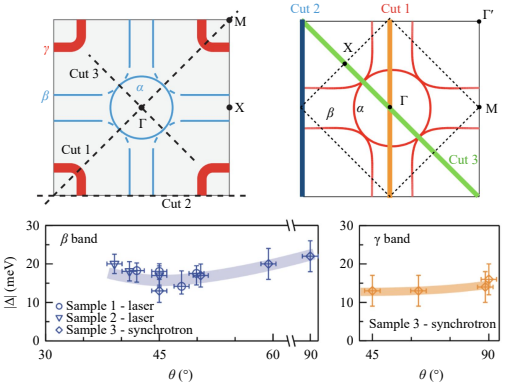

Keywords nickelate superconductors, thin films, ambient pressure, transition temperature, electronic structure, pairing symmetry

Contents

*Special Topic: Celebrating the 20th Anniversary of the Founding of Frontiers of Physics (Eds.: Zhimin Liao, Jun He & Huabing Yang).

1 Introduction

Since the discovery of superconductivity (SC) in copper oxides with a transition temperature (T_c) of up to 164 K [1, 2], many efforts have been devoted to finding more high-T_c superconductors. One of the promising candidates predicted to be a high-T_c superconductor is nickel oxides, as nickel is located next to copper in the periodic table and is therefore believed to possess similar properties [3]. In 2019, the prediction was finally confirmed with the discovery of SC in an infinite-layer nickelate [4]. In 2023, Sun *et al.* [5] found SC with T_c near 80 K in bilayer nickelate $La_3Ni_2O_7$ under high pressure, marking nickelates as the second class of high-T_c superconductor to enter the liquid-nitrogen temperature range, following copper oxides. In 2024, Zhu *et al.* [6–8] observed SC

https://doi.org/10.15302/frontphys.2026.115301

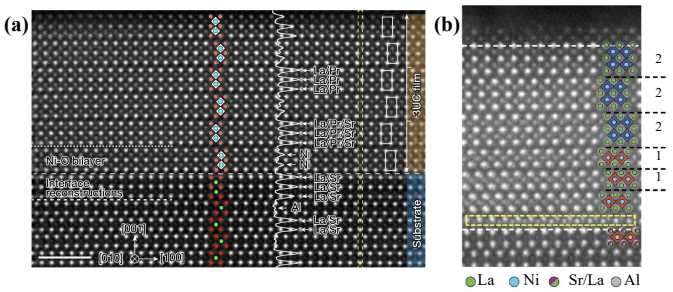

Fig. 1 Microscopic structures of **(a)** $La_{2.85}Pr_{0.15}Ni_2O_7$ sample on $SrLaAlO_4$ [10] and **(b)** of $La_3Ni_2O_7$ on $SrLaAlO_4$ [9].

with $T_c = 20$–30 K under high pressure in trilayer nickelate $La_4Ni_3O_{10}$, further expanding the family of nickelate superconductors. However, the requirement of high pressure has significantly limited the use of specific key experimental techniques for directly investigating the superconducting phase. Consequently, considerable research has focused on achieving ambient-pressure SC in nickelates.

Recently, using pulsed laser deposition (PLD), Ko *et al.* [9] reported ambient-pressure SC with a T_c exceeding 40 K in $La_3Ni_2O_7$ thin films grown on $SrLaAlO_4$ (SLAO) substrates. Almost simultaneously, Zhou *et al.* [10] independently observed ambient-pressure SC with a T_c over 40 K in $La_{2.85}Pr_{0.15}Ni_2O_7$ thin films grown on the same substrates by gigantic-oxidative atomic-layer-by-layer epitaxy (GAE) [11, 12]. And many experiments have been conducted on the samples synthesized by GAE [13–15]. The microscopic structures of these thin films are shown in Fig. 1. Later, several groups reported ambient-pressure SC in related systems, including $La_2PrNi_2O_7$ [16–18], and $La_{3-x}Sr_xNi_2O_7$ thin films [19–21]. And more and more $La_3Ni_2O_7$ thin-film samples are synthesized and various experimental explorations have been conducted on them until right now [22–25]. And among these findings, the effect of element doping on $La_3Ni_2O_7$ thin films has been investigated systematically. Partial substitution of La with Pr in $La_3Ni_2O_7$ has been reported to improve sample quality, enhancing phase purity and SC [10, 16]. The effect of carrier doping is studied through Sr^{2+} doping in $La_{3-x}Sr_xNi_2O_7$, which serves as an equivalent approach for hole doping, giving a phase diagram where the highest T_c value of 42 K is achieved at $x = 0.21$ [19]. These findings represent a significant advancement in the field of nickelate superconductors.

In this review, we begin by examining the role of epitaxial strain in enabling ambient-pressure SC in $La_3Ni_2O_7$ thin films. We then examine key experimental studies, especially ARPES measurements that reveal distinct Fermi surface (FS) topologies, and summarize methods for raising the superconducting transition temperature T_c. Finally, we review recent theoretical studies of the electronic structures and possible pairing symmetry in $La_3Ni_2O_7$ thin films.

2 Effects of epitaxial strain

To achieve ambient-pressure SC, one promising approach is to apply epitaxial strain to $La_3Ni_2O_7$ thin films. Before discussing the effects of epitaxial strain, it is necessary to analyze the pressure phase diagram of bulk $La_3Ni_2O_7$ [26], which can be divided into a low-pressure region (LP) and a high-pressure region (HP). The characteristic structure of $La_3Ni_2O_7$ is its bilayer NiO_2 planes, where each layer contains a NiO_6 octahedron [27, 28]. The two octahedra share an apical oxygen, forming a Ni-O-Ni bond. In the LP phase, the space group is *Aman*, characterized by a 168° bond angle. As the pressure approaches approximately 10 GPa, it transitions into the HP phase, characterized by two octahedra aligned with each other, leading to a bond angle tilting to 180° and the space group changing to *Fmmm* above 14 GPa and *I*4/*mmm* above 46.8 GPa.

Since SC only appears in the HP phase, the main challenge is to stabilize this HP phase in thin films at ambient pressure. Cui *et al.* [29] revealed that epitaxial misfit strain is the dominant factor controlling the phase formation in RP nickelates $La_{n+1}Ni_nO_{3n+1}$. Their report indicates that tensile strain stabilizes the perovskite $LaNiO_3$ ($n = \infty$) phase, while compressive strain favors the formation of the $La_3Ni_2O_7$ ($n = 2$) phase. Therefore, substrates play an important role in the induction of SC in bilayer nickelate thin films. As shown in Fig. 2(a), the temperature-dependent resistivity $\rho(T)$ of $La_3Ni_2O_7$ thin films grown on SLAO substrates begins to decrease at approximately 42 K and reaches zero resistance near 2 K. In contrast, $\rho(T)$ for films grown on $LaAlO_3$ (LAO) and $(LaAlO_3)_{0.3}(Sr_2TaAlO_6)_{0.7}$ (LSAT) substrates shows an upturn below 40 K without reaching a zero-resistance state [9]. The main difference among these substrates comes from their in-plane lattice constants, with SLAO applying compressive strain, LAO exerting only a mild compressive strain, and LSAT introducing a slight tensile strain. These results demonstrate that compressive strain is crucial for inducing ambient-pressure SC in $La_3Ni_2O_7$ thin films. In addition, the results from Chen's group showed that the transition to zero resistance exhibits signatures of a Berezinskii–Kosterlitz–Thouless (BKT) transition [10].

3 Characterization results

The absence of high-pressure requirements in these thin films enables direct experimental investigation of the superconducting phase. Consequently, various measurements have been performed on bilayer nickelate thin films to investigate the underlying mechanisms of SC.

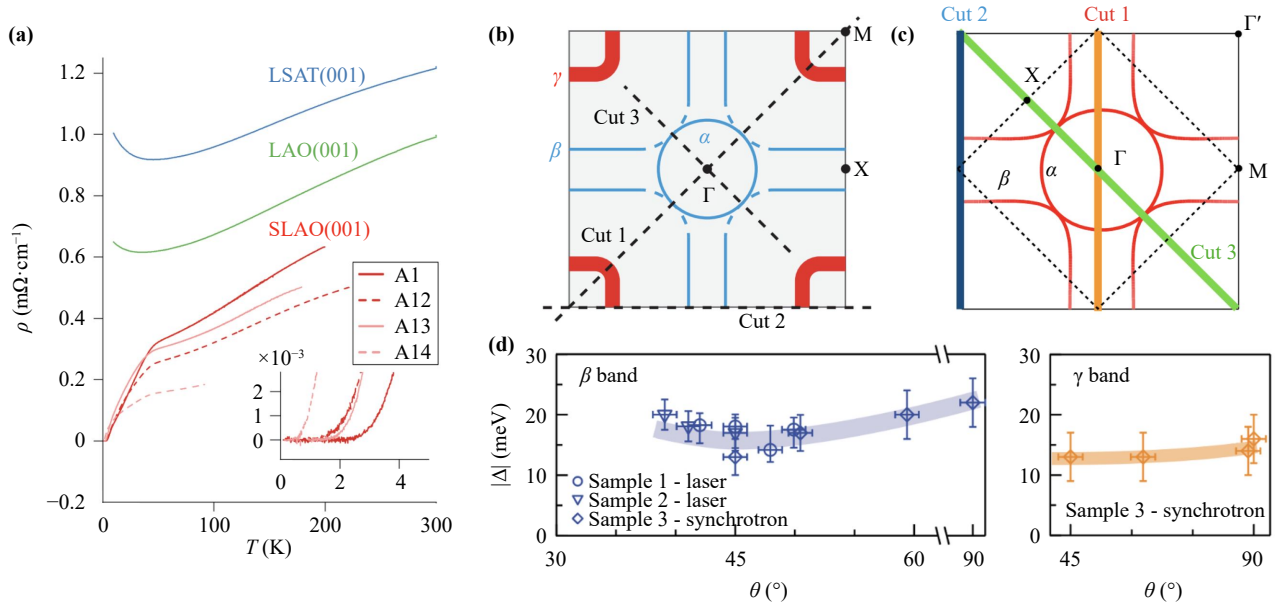

Fig. 2 **(a)** Temperature-dependent resistivity $\rho(T)$ of $La_3Ni_2O_7$ thin films grown on different substrates [9]. **(b)** FS of $La_{2.85}Pr_{0.15}Ni_2O_7$ thin films, consisting of α, β and γ pockets [13]. **(c)** FS of $La_2PrNi_2O_7$ thin films, without γ pocket appearing on FS [17]. **(d)** Measured superconducting gap magnitudes on the β and γ bands as a function of the angle θ [24].

Scanning transmission electron microscopy (STEM) measurements show that the apical Ni–O–Ni bond angle approaches 180° [9], which is very similar to the HP phase of bulk $La_3Ni_2O_7$. It is also notable that ozone annealing plays an important role in ambient SC of $La_3Ni_2O_7$ thin films. After O_3 annealing, the as-grown $La_3Ni_2O_7$ thin films transition from an insulating state into a superconducting state [9]. And the X-ray absorption spectroscopy (XAS) measurements further indicate that the O_3-annealed thin films contain a combination of 50% Ni^{2+} and 50% Ni^{3+}, whereas the as-grown thin films contain 55% Ni^{2+} and 45% Ni^{3+} [9]. Thus, the Ni ion in the O_3-annealed thin films exhibits a mixed valence state of 2.5. These facts show that ozone annealing can increase oxygen content, and maintain a $Ni^{2.5+}$ valence state in $La_3Ni_2O_7$ thin films. Angle-resolved photoemission spectroscopy (ARPES) studies [13, 17, 24] on bilayer nickelate thin films have been conducted to confirm the topology of FS. As shown in Fig. 2(b), ARPES measurements on $La_{2.85}Pr_{0.15}Ni_2O_7$ thin films [13] reveal a FS, where the α, β and γ pockets are identified. Furthermore, direct measurement of the superconducting gap on the FS [24] reveals a significant gap opening on the β FS sheet with no signs of nodes along the Brillouin-zone diagonal, as shown in Fig. 2(d). Notably, this gap survives to a temperature above T_c and shows a particle–hole symmetric evolution, consistent with the presence of a pseudogap. However, ARPES measurements on $La_2PrNi_2O_7$ thin films [17] give a FS without the γ pocket, which is about 70 meV below the Fermi level, as shown in Fig. 2(c). ARPES measurements on Sr-doped $La_3Ni_2O_7$ thin films also reports a FS without the γ pocket [20]. The contrast results may arise from differences in the growth conditions and measurement environment of the thin films. It has been reported that Sr diffusion from substrates was observed, which may also result in the appearance of the γ pocket [13]. Whether γ pocket appears in the intrinsic $La_3Ni_2O_7$ thin films under 2% compressive strain is still under debate. Scanning tunneling microscopy (STM) measurements [18] reveal a two-gap structure on the FS, with fitting analyses indicating a preferred anisotropic s-wave pairing. Taken together, these observations support a predominant $s\pm$-wave pairing symmetry in the system. But whether the pairing symmetry is $s^{\pm}$ wave is still under debate. Most recently, Nie *et al.* [14] reported ambient-pressure SC with onset T_c up to 50 K in both hybrid monolayer-bilayer (1212) and pure bilayer (2222) films, and onset T_c of 46 K in bilayer–trilayer (2323) thin films, while the hybrid monolayer-trilayer (1313) structure remained non-superconducting. The FS of these films measured by ARPES in Fig. 3 showed a clear difference: a hole-like γ band crosses the Fermi level in the superconducting films, but in the non-superconducting 1313 film, it is below the Fermi level. A recent theoretical work attributes the suppression of SC in 1313 $La_3Ni_2O_7$ to reduced pairing strength in the trilayer subsystem and weakened phase coherence between trilayer subsystems arising from S–N–S Josephson coupling [30].

4 Methods to increase T_c

Following the discovery of SC in bulk and thin-film

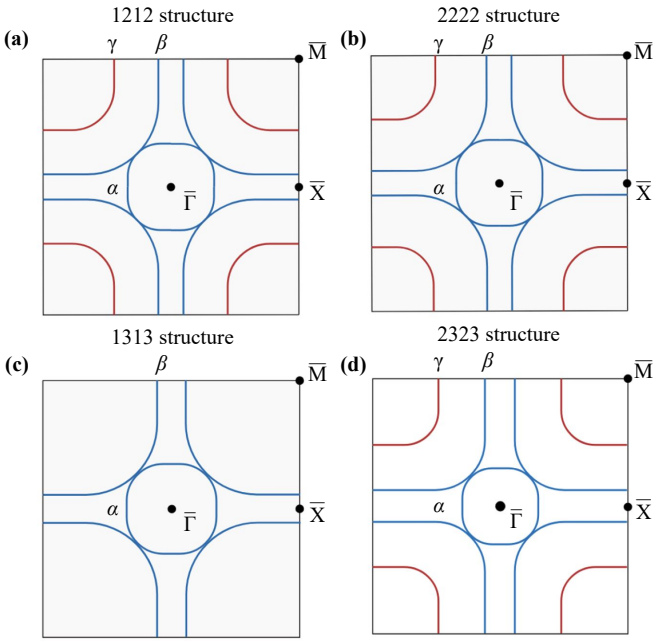

Fig. 3 FS [14] of thin films grown on SLAO substrates measured by ARPES for **(a)** 1212 structure, **(b)** 2222 structure, **(c)** 1313 structure and **(d)** 2323 structure.

$La_3Ni_2O_7$, methods to raise T_c have emerged as a major research focus. In thin film systems, methods to increase T_c mainly involve enhancing thin-film growth techniques and applying pressure. Zhou *et al.* [15] showed that their improved GAE technique, achieved by pushing the growth regime into an extreme non-equilibrium state, can stabilize an ambient-pressure superconducting phase with an onset temperature of up to 63 K. Osada *et al.* [23] showed that as the c/a ratio increases, the onset T_c under hydrostatic pressure rises from approximately 10 K under tensile strain to nearly 60 K under compressive strain. Applying hydrostatic pressure on compressively strained $La_3Ni_2O_7$ thin films, which raises the onset T_c to over 60 K, has also been reported recently [31]. And most recently, Zhao *et al.* [32] showed that hydrostatic pressure universally enhances SC in $(La,Pr)_3Ni_2O_7$ thin films, raising the onset T_c to 68.5 K at 2.0 GPa. They attribute the observed resistance dip above T_c to oxygen-vacancy-induced electron localization. The dip is suppressed by pressure, which directly correlates with the increase in T_c, establishing oxygen vacancies as a key tuning parameter for SC in bilayer nickelates. Overall, T_c in thin films is probably enhanced by pressure via increasing interlayer coupling, orbital hybridization, and spin fluctuations. Also, some theoretical works [33, 34] have explored methods to enhance T_c by applying an electric field to thin films, which require experimental verification. While in bulk systems, using element substitution to increase T_c [35] has advanced significantly. In bulk systems, Li *et al.* [36] reported bulk SC in $La_2SmNi_2O_7$ under high pressure, which exhibits a T_c up to 96 K, zero resistance temperature up to 73 K, and clear Meissner screening, confirming robust bulk high-T_c behavior. Qiu *et al.* [37] demonstrated that Nd substitution in bilayer $La_3Ni_2O_7$ compresses the lattice and enhances interlayer magnetic coupling, resulting in SC with an onset T_c of up to approximately 98 K. Chen *et al.* [38] systematically calculated the electronic structures of Nd-doping bulk $La_3Ni_2O_7$, revealing that increasing Nd doping leads to a larger interlayer d_{z^2} orbital hopping, which would result in a larger interlayer superexchange coupling and a higher T_c. In conclusion, rare-earth element substitutions can induce chemical pressure in bulk $La_3Ni_2O_7$ to raise T_c. It has been reported that applying pressure can increase T_c in thin films [31], suggesting that T_c might be enhanced by chemical pressure. The effectiveness of this approach needs further experimental verification.

5 Theory progress of bilayer nickelate thin films

Since the discovery of SC in bilayer nickelate thin films, significant focus has been directed toward their underlying electronic structures. Several research groups subsequently performed systematic calculations of the electronic band structures [16, 22, 39, 40, 43, 44], employing first-principles density functional theory (DFT) and model analyses to characterize the low-energy states, FS topology, and orbital composition [45]. Using the constrained random phase approximation (cRPA), Yue *et al.* [39] demonstrated intra-orbital Coulomb interaction $U \approx 3.77$ eV and Hund's coupling $J_H \approx 0.56$ eV. Combining DFT and dynamical mean-field theory (DMFT) with the U and J_H obtained from cRPA and a particle filling of $n = 1.3$, they reproduced FS comparable to ARPES results, as shown in Figs. 4(a) and (c). Using DFT, Hu *et al.* [40] systematically investigated the electronic structures and slab models across various thicknesses. They constructed the One-UC (unit cell) double-stack tight-binding model and the Half-UC slab model, which is used for comparison, and proposed a double-stack high-energy d–p model for the first time, laying the groundwork for future research. The energy bands and FS of the One-UC double-stack tight-binding model are shown in Figs. 4(b) and (d). Since the One-UC slab consists of two bilayers, there is some small hopping between the two bilayers, resulting in a small split of the γ pocket. It is notable that the interlayer d_{z^2} orbital hopping parameter for the One-UC slab is –0.550, while for the Half-UC slab it is –0.503. This suggests that the One-UC slab may have a larger interlayer d_{z^2} orbital superexchange coupling compared to the Half-UC case, according to $J \sim 4t^2/U$. Based on the double-stack model, the random phase approximation (RPA) spin susceptibility exhibits the strongest response reflecting nesting intra γ pocket.

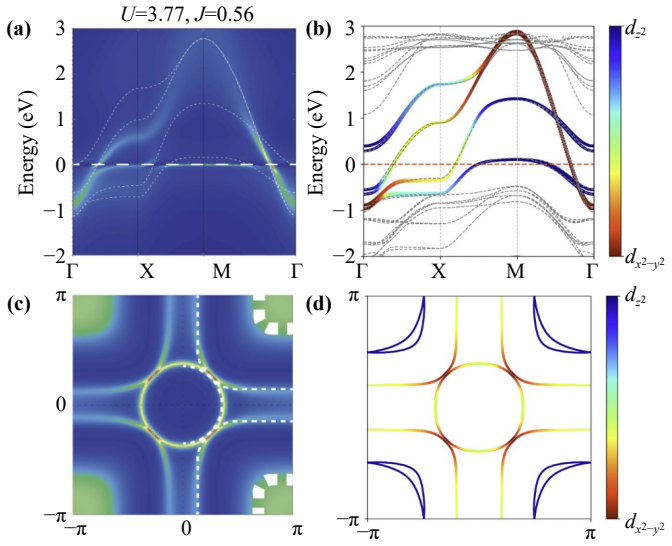

Fig. 4 **(a)** The energy bands and **(c)** FS of $La_3Ni_2O_7$ thin films, combining DFT and DMFT [39]. **(b)** The energy bands and **(d)** FS of the One-UC double-stack tight-binding model for $La_3Ni_2O_7$ thin films [40].

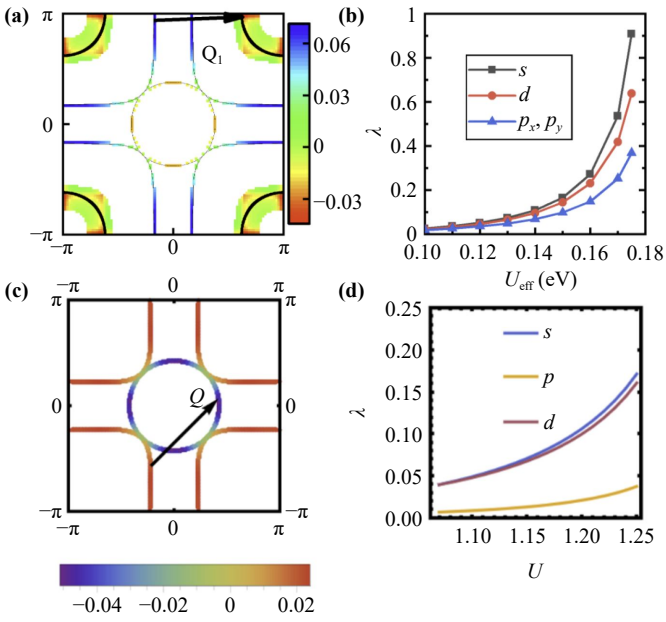

Fig. 5 **(a)** The leading cRPA calculated gap functions on the FS and **(b)** the dependence of λ on U_{eff} [39]. **(c)** The leading RPA calculated gap functions on the FS and **(d)** the dependence of λ on U without γ pocket [41].

Building on a similar double-stack model, Li *et al.* [46] performed a DFT+U study of $La_3Ni_2O_7/SrLaAlO_4$ thin films, explicitly incorporating both substrate-induced compressive strain and interfacial Sr interdiffusion. Recently, using DQMC and DMFT, Zhong *et al.* [47] reported that, $La_3Ni_2O_7$ thin films exhibit a significantly enhanced charge-transfer capability together with interlayer and intralayer antiferromagnetic correlations of comparable magnitude.

Pairing symmetry is an important question in high-T_c superconductors. Weak-coupling methods, such as RPA [48, 49] and functional renormalization group (FRG) [50, 51], are typically used to find out the pairing symmetry. Yue *et al.* [39] used a modified RPA approach based on their model, resulting in an $s^{\pm}$ wave pairing symmetry, as shown in Figs. 5(a) and (b). However, the RPA approach is very sensitive to the details of FS. Shao *et al.* [41] constructed a tight-binding model without γ pocket, giving rise to an $s^{\pm}$ wave pairing symmetry, driven by nesting between the α pocket and β pocket, as shown in Figs. 5(c) and (d). A work using the variational Monte Carlo method also reports a robust $s^{\pm}$ symmetry against change in FS [52]. Combining first-principles and FRG calculations, Le *et al.* [43] found that scattering between FS sheets with opposite parity symmetry enhances interlayer $s^{\pm}$ wave SC, while nesting between FS sheets with the same parity symmetry would break the pairing. Using FRG, Cao *et al.* [53] found that the pairing symmetry for both $La_3Ni_2O_7$ and $La_{2.85}Pr_{0.15}Ni_2O_7$ thin films is $s^{\pm}$ wave and T_c could be enhanced under in-plane compression. Recently, Zhang *et al.* [54] used the RPA approach on a one-UC compressive $La_3Ni_2O_7$ thin film, revealing a leading $d_{x^2-y^2}$ pairing state at moderate hole doping, and a d_{xy} pairing symmetry with higher doping level. However, there are also some works supporting d_{xy} wave or $d+is$ symmetry [55, 56]. And a recent measurement of differential conductance (dI/dV) spectra on pressurized $La_3Ni_2O_{7-\delta}$ single crystal suggests a d-wave-like symmetry [57]. Another theoretical method for identifying the pairing symmetry is the renormalized mean-field theory (RMFT) [58, 59], which begins with the $t-J$ model. Qiu *et al.* [42] used the $t-J$ Hamiltonian, including superexchange couplings $J_{\perp}^{z}$, $J_{||}^{x}$, J_{xz}, and $J_{\rm H}$, to investigate the pairing symmetry and superconducting gap structure on the FS in $La_3Ni_2O_7$ thin films. Using exact diagonalization, the authors estimated $J_{\perp}^{z} \approx 0.135$ eV. The resulting superconducting gap projected on the FS is shown in Fig. 6(a), indicating a nodal $s^{\pm}$ wave pairing symmetry. The angular dependences of the gap on different pockets are shown in Figs. 6(b)–(d). The gaps on the β and γ pockets are nodeless and have opposite signs, while a sign change occurs on the α pocket. Whether there are nodes on the α pocket still needs more experimental results to prove. On the β pocket, the gap shows a parabolic shape centered around 45°, and it slightly decreases as it nears the corner. Orbital-resolved superconducting gaps are displayed in Figs. 6(e)–(h). Qiu *et al.* [42] systematically studied the phase patterns and pointed out that they can be interpreted as maximizing the overall gap magnitude on FS. As a result, $\Delta_{||}^{z}$ tends to maximize the gap on the γ pocket, whereas $\Delta_{||}^{x}$ enhances the gap on the α pocket, with only minor suppression on the β pocket. Moreover, as temperature

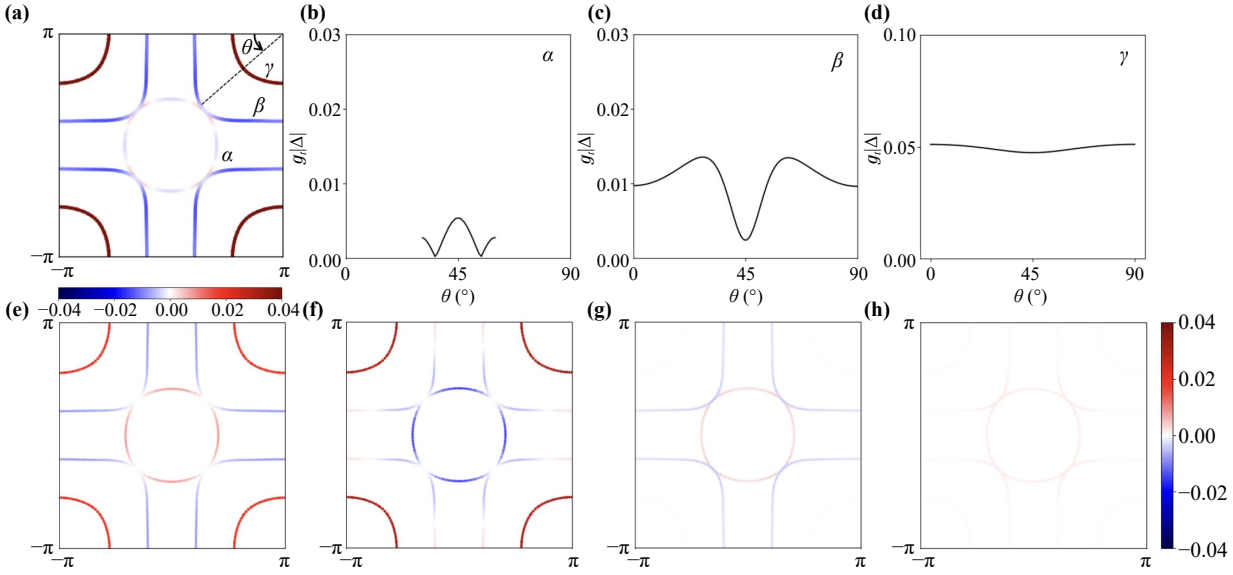

Fig. 6 **(a)** Superconducting gap projected on the FS and **(b–d)** superconducting gap as a function of angle for α, β and γ pockets, respectively. **(e–h)** Orbital-resolved superconducting gap on the FS for interlayer d_{z^2}, inplane d_{z^2}, interlayer $d_{x^2-y^2}$ and inplane $d_{x^2-y^2}$ pairing, respectively [42].

rises, the energy gap of all pairing bonds decreases to zero at approximately 60 K in a mean-field manner. Recently, some researchers have paid attention to the prediction of the T_c in superconductors [60, 61]. They tried to explore intrinsic constraints on the T_c in unconventional superconductors [60] and give an empirical scaling relation connecting the maximum T_c^* to the effective on-site Coulomb interaction U in unconventional superconductors [61]. While the relation appears robust across some correlated superconductors, its microscopic origin remains an open question.

6 Summary

To date, some issues still need clarification. First, the role of the γ pocket in enabling SC in bilayer nickelate thin films remains to be fully clarified. Second, the relationship between the lattice ratio c/a and the superconducting transition temperature T_c in thin films differs from that in bulk $La_3Ni_2O_7$. These unresolved and seemingly contradictory results highlight the need for further experimental work to better understand SC in bilayer nickelate thin films.

Declarations The authors declare that they have no competing interests and there are no conflicts.

Acknowledgements We are grateful to Zhihui Luo and Cui-Qun Chen for useful discussions. Work at Sun Yat-sen University was supported by the National Natural Science Foundation of China (Grant Nos. 12494591 and 92565303), the National Key Research and Development Program of China (Grant No. 2022YFA1402802), the Guangdong Provincial Key Laboratory of Magnetoelectric Physics and Devices (No. 2022B1212010008), the Research Center for Magnetoelectric Physics of Guangdong Province (No. 2024B0303390001), and the Guangdong Provincial Quantum Science Strategic Initiative (Grant No. GDZX2401010).

References

1. J. G. Bednorz and K. A. Müller, Possible high T_c superconductivity in the Ba–La–Cu–O system, *Z. Phys. B* 64(2), 189 (1986)
2. L. Gao, Y. Y. Xue, F. Chen, Q. Xiong, R. L. Meng, D. Ramirez, C. W. Chu, J. H. Eggert, and H. K. Mao, Superconductivity up to 164 K in $HgBa_2Ca_{m-1}Cu_mO_{2m+2+\delta}$ (m=1, 2, and 3) under quasi-hydrostatic pressures, *Phys. Rev. B* 50(6), 4260 (1994)
3. V. I. Anisimov, D. Bukhvalov, and T. M. Rice, Electronic structure of possible nickelate analogs to the cuprates, *Phys. Rev. B* 59(12), 7901 (1999)
4. D. Li, K. Lee, B. Y. Wang, M. Osada, S. Crossley, H. R. Lee, Y. Cui, Y. Hikita, and H. Y. Hwang, Superconductivity in an infinite-layer nickelate, *Nature* 572(7771), 624 (2019)
5. H. Sun, M. Huo, X. Hu, J. Li, Z. Liu, Y. Han, L. Tang, Z. Mao, P. Yang, B. Wang, J. Cheng, D. X. Yao, G. M. Zhang, and M. Wang, Signatures of superconductivity near 80 K in a nickelate under high pressure, *Nature* 621(7979), 493 (2023)
6. Y. Zhu, D. Peng, E. Zhang, B. Pan, X. Chen, L. Chen, H. Ren, F. Liu, Y. Hao, N. Li, Z. Xing, F. Lan, J. Han, J. Wang, D. Jia, H. Wo, Y. Gu, Y. Gu, L. Ji, W. Wang, H. Gou, Y. Shen, T. Ying, X. Chen, W. Yang, H. Cao, C. Zheng, Q. Zeng, J. Guo, and J. Zhao, Superconductivity in pressurized trilayer $La_4Ni_3O_{10-\delta}$ single crystals, *Nature* 631(8021), 531 (2024)

7. Q. Li, Y. J. Zhang, Z. N. Xiang, Y. Zhang, X. Zhu, and H. H. Wen, Signature of superconductivity in pressurized $La_4Ni_3O_{10}$, *Chin. Phys. Lett.* 41(1), 017401 (2024)
8. M. Zhang, C. Pei, D. Peng, X. Du, W. Hu, Y. Cao, Q. Wang, J. Wu, Y. Li, H. Liu, C. Wen, J. Song, Y. Zhao, C. Li, W. Cao, S. Zhu, Q. Zhang, N. Yu, P. Cheng, L. Zhang, Z. Li, J. Zhao, Y. Chen, C. Jin, H. Guo, C. Wu, F. Yang, Q. Zeng, S. Yan, L. Yang, and Y. Qi, Superconductivity in trilayer nickelate $La_4Ni_3O_{10}$ under pressure, *Phys. Rev. X* 15(2), 021005 (2025)
9. E. K. Ko, Y. Yu, Y. Liu, L. Bhatt, J. Li, V. Thampy, C. T. Kuo, B. Y. Wang, Y. Lee, K. Lee, J. S. Lee, B. H. Goodge, D. A. Muller, and H. Y. Hwang, Signatures of ambient pressure superconductivity in thin film $La_3Ni_2O_7$, *Nature* 638(8052), 935 (2025)
10. G. Zhou, W. Lv, H. Wang, Z. Nie, Y. Chen, Y. Li, H. Huang, W. Chen, Y. Sun, Q. K. Xue, and Z. Chen, Ambient-pressure superconductivity onset above 40 K in $(La, Pr)_3Ni_2O_7$ films, *Nature* 640(8059), 641 (2025)
11. M. Kanai, T. Kawai, S. Kawai, and H. Tabata, Low-temperature formation of multilayered Bi(Pb)–Sr–Ca–Cu– O thin films by successive deposition using laser ablation, *Appl. Phys. Lett.* 54(18), 1802 (1989)
12. G. Zhou, H. Huang, F. Wang, H. Wang, Q. Yang, Z. Nie, W. Lv, C. Ding, Y. Li, J. Lin, C. Yue, D. Li, Y. Sun, J. Lin, G. M. Zhang, Q. K. Xue, and Z. Chen, Gigantic-oxidative atomic-layer-by-layer epitaxy for artificially designed complex oxides, *Natl. Sci. Rev.* 12(4), nwae429 (2025)
13. P. Li, G. Zhou, W. Lv, Y. Li, C. Yue, H. Huang, L. Xu, J. Shen, Y. Miao, W. Song, Z. Nie, Y. Chen, H. Wang, W. Chen, Y. Huang, Z. H. Chen, T. Qian, J. Lin, J. He, Y. J. Sun, Z. Chen, and Q. K. Xue, Angle-resolved photoemission spectroscopy of superconducting $(La, Pr)_3Ni_2O_7/SrLaAlO_4$ heterostructures, *Natl. Sci. Rev.* 12(10), nwaf205 (2025)
14. Z. Nie, Y. Li, W. Lv, L. Xu, Z. Jiang, P. Fu, G. Zhou, W. Song, Y. Chen, H. Wang, H. Huang, J. Lin, J. F. Jia, D. Shen, P. Li, Q. K. Xue, and Z. Chen, Superconductivity and electronic structures of nickelate thin film superstructures, *Nature* 652(8110), 628 (2026)
15. G. Zhou, H. Wang, H. Huang, Y. Chen, F. Peng, W. Lv, Z. Nie, W. Wang, J. F. Jia, Q. K. Xue, and Z. Chen, Superconductivity onset above 60 K in ambient-pressure nickelate films, *Natl. Sci. Rev.* 2026, nwag151 (2026)
16. Y. Liu, E. K. Ko, Y. Tarn, L. Bhatt, J. Li, V. Thampy, B. H. Goodge, D. A. Muller, S. Raghu, Y. Yu, and H. Y. Hwang, Superconductivity and normal-state transport in compressively strained $La_2PrNi_2O_7$ thin films, Nat, *Mater.* 24, 1221 (2025)
17. B. Y. Wang, Y. Zhong, S. Abadi, Y. Liu, Y. Yu, X. Zhang, Y. M. Wu, R. Wang, J. Li, Y. Tarn, E. K. Ko, V. Thampy, M. Hashimoto, D. Lu, Y. S. Lee, T. P. Devereaux, C. Jia, H. Y. Hwang, and Z. X. Shen, Electronic structure of compressively strained thin film $La_2PrNi_2O_7$, arXiv: 2504.16372 (2025)
18. S. Fan, M. Ou, M. Scholten, Q. Li, Z. Shang, Y. Wang, J. Xu, H. Yang, I. M. Eremin, and H. H. Wen, Superconducting gap structure and bosonic mode in $La_2PrNi_2O_7$ thin films at ambient pressure, arXiv: 2506.01788 (2025)
19. B. Hao, M. Wang, W. Sun, Y. Yang, Z. Mao, S. Yan, H. Sun, H. Zhang, L. Han, Z. Gu, J. Zhou, D. Ji, and Y. Nie, Superconductivity in Sr-doped $La_3Ni_2O_7$ thin films, *Nat. Mater.* 24(11), 1756 (2025)
20. W. Sun, Z. Jiang, B. Hao, S. Yan, H. Zhang, M. Wang, Y. Yang, H. Sun, Z. Liu, D. Ji, Z. Gu, J. Zhou, D. Shen, D. Feng, and Y. Nie, Observation of superconductivity-induced leading-edge gap in Sr-doped $La_3Ni_2O_7$ thin films, arXiv: 2507.07409 (2025)
21. H. Zhong, B. Hao, A. Chen, X. Huang, C. Li, W. Zhang, C. Liu, K. Kummer, N. Brookes, Y. Nie, T. Schmitt, and X. Lu, Doping evolution of spin excitations in $La_{3-x}Sr_xNi_2O_7/SrLaAlO_4$ superconducting thin films, arXiv: 2603.01120 (2026)
22. L. Bhatt, A. Y. Jiang, E. K. Ko, N. Schnitzer, G. A. Pan, D. F. Segedin, Y. Liu, Y. Yu, Y. F. Zhao, E. A. Morales, C. M. Brooks, A. S. Botana, H. Y. Hwang, J. A. Mundy, D. A. Muller, and B. H. Goodge, Resolving structural origins for superconductivity in strain-engineered $La_3Ni_2O_7$ thin films, arXiv: 2501.08204 (2025)
23. M. Osada, C. Terakura, A. Kikkawa, M. Nakajima, H. Y. Chen, Y. Nomura, Y. Tokura, and A. Tsukazaki, Strain-tuning for superconductivity in $La_3Ni_2O_7$ thin films, *Commun. Phys.* 8(1), 251 (2025)
24. J. Shen, G. Zhou, Y. Miao, P. Li, Z. Ou, Y. Chen, Z. Wang, R. Luan, H. Sun, Z. Feng, X. Yong, Y. Li, L. Xu, W. Lv, Z. Nie, H. Wang, H. Huang, Y. J. Sun, Q. K. Xue, J. He, and Z. Chen, Nodeless superconducting gap and electron–boson coupling in $(La, Pr, Sm)_3Ni_2O_7$ films, arXiv: 2502.17831 (2025)
25. H. Ji, Z. Xie, Y. Chen, G. Zhou, L. Pan, H. Wang, H. Huang, J. Ge, Y. Liu, G. M. Zhang, Z. Wang, Q. K. Xue, Z. Chen, and J. Wang, Time-reversal symmetry breaking superconductivity with electronic glass in nickelate $(La,Pr,Sm)_3Ni_2O_7$ films, arXiv: 2508.16412 (2026)
26. J. Li, D. Peng, P. Ma, H. Zhang, Z. Xing, X. Huang, C. Huang, M. Huo, D. Hu, Z. Dong, X. Chen, T. Xie, H. Dong, H. Sun, Q. Zeng, H. Mao, and M. Wang, Identification of superconductivity in bilayer nickelate $La_3Ni_2O_7$ under high pressure up to 100 GPa, *Natl. Sci. Rev.* 12(10), nwaf220 (2025)
27. M. Wang, H. H. Wen, T. Wu, D. X. Yao, and T. Xiang, Normal and superconducting properties of $La_3Ni_2O_7$, *Chin. Phys. Lett.* 41(7), 077402 (2024)
28. Y. Wang, K. Jiang, J. Ying, T. Wu, J. Cheng, J. Hu, and I. Chen, Recent progress in nickelate superconductors, *Natl. Sci. Rev.* 12(10), nwaf373 (2025)
29. T. Cui, S. Choi, T. Lin, C. Liu, G. Wang, N. Wang, S. Chen, H. Hong, D. Rong, Q. Wang, Q. Jin, J. O. Wang, L. Gu, C. Ge, C. Wang, J. G. Cheng, Q. Zhang, L. Si, K. Jin, and E. J. Guo, Strain-mediated phase crossover in Ruddlesden–Popper nickelates, *Commun. Mater.* 5(1), 32 (2024)
30. C. Q. Chen, M. Zhang, F. Yang, and D. X. Yao, Pairing mechanism and superconductivity in 1313 phase $La_3Ni_2O_7$, arXiv: 2604.21533 (2026)
31. Q. Li, J. Sun, S. Bötzel, M. Ou, Z. N. Xiang, F. Lechermann, B. Wang, Y. Wang, Y. J. Zhang, J. Cheng, I. M. Eremin, and H. H. Wen, Enhanced superconductivity in the compressively strained bilayer nickelate thin films by pressure, *Nat. Commun.* 17(1), 3276 (2026)
32. J. Zhao, G. Zhou, S. Cai, S. Sun, Y. Chen, J. Guo, Y. Zhou, H. Huang, J. F. Jia, Y. Ding, Q. Wu, Z. Chen, Q. K. Xue, and L. Sun, Pressure-enhanced superconductivity

and its correlation with suppressed resistance dip in $(La, Pr)_3Ni_2O_7$ films, arXiv: 2603.29531 (2026)
33. Z. Y. Shao, J. H. Ji, C. Wu, D. X. Yao, and F. Yang, Possible liquid-nitrogen-temperature superconductivity driven by perpendicular electric field in the single-bilayer film of $La_3Ni_2O_7$ at ambient pressure, *Nat. Commun.* 17(1), 17 (2026)
34. Z. D. Fan and A. Vishwanath, Minimal two band model and experimental proposals to distinguish pairing mechanisms of the high-T_c superconductor $La_3Ni_2O_7$, arXiv: 2512.05956 (2025)
35. Z. Pan, C. Lu, F. Yang, and C. Wu, Effect of rare-earth element substitution in superconducting $R_3Ni_2O_7$ under pressure, *Chin. Phys. Lett.* 41(8), 087401 (2024)
36. F. Li, Z. Xing, D. Peng, J. Dou, N. Guo, L. Ma, Y. Zhang, L. Wang, J. Luo, J. Yang, J. Zhang, T. Chang, Y. S. Chen, W. Cai, J. Cheng, Y. Wang, Y. Liu, T. Luo, N. Hirao, T. Matsuoka, H. Kadobayashi, Z. Zeng, Q. Zheng, R. Zhou, Q. Zeng, X. Tao, and J. Zhang, Bulk superconductivity up to 96 K in pressurized nickelate single crystals, *Nature* 649(8098), 871 (2026)
37. Z. Qiu, J. Chen, D. V. Semenok, Q. Zhong, D. Zhou, J. Li, P. Ma, X. Huang, M. Huo, T. Xie, and X. Chen, H. kwang Mao, V. Struzhkin, H. Sun, and M. Wang, Interlayer coupling enhanced superconductivity near 100 K in $La_{3-x}Nd_xNi_2O_7$, arXiv: 2510.12359 (2025)
38. C. Q. Chen, W. Qiu, Z. Luo, M. Wang, and D. X. Yao, Electronic structures and superconductivity in Nd-doped $La_3Ni_2O_7$, *Sci. China Phys. Mech. Astron.* 69(4), 247414 (2026)
39. C. Yue, J. J. Miao, H. Huang, Y. Hua, P. Li, Y. Li, G. Zhou, W. Lv, Q. Yang, F. Yang, H. Sun, Y. J. Sun, J. Lin, Q. K. Xue, Z. Chen, and W. Q. Chen, Correlated electronic structures and unconventional superconductivity in bilayer nickelate heterostructures, *Natl. Sci. Rev.* 12(10), nwaf253 (2025)
40. X. Hu, W. Qiu, C. Q. Chen, Z. Luo, and D. X. Yao, Electronic structures and multi-orbital models of $La_3Ni_2O_7$ thin films at ambient pressure, *Commun. Phys.* 8(1), 506 (2025)
41. Z. Y. Shao, C. Lu, M. Liu, Y. B. Liu, Z. Pan, and C. Wu, and F. Yang, Pairing without γ-pocket in the $La_3Ni_2O_7$ thin film, arXiv: 2507.20287 (2025)
42. W. Qiu, Z. Luo, X. Hu, and D. X. Yao, Pairing symmetry and superconductivity in $La_3Ni_2O_7$ thin films, arXiv: 2506.20727 (2025)
43. C. Le, J. Zhan, X. Wu, and J. Hu, Opposite-mirror-parity scattering as the origin of superconductivity in strained bilayer nickelates, arXiv: 2501.14665 (2025)
44. H. Shi, Z. Huo, G. Li, H. Ma, T. Cui, D. X. Yao, and D. Duan, The effect of carrier doping and thickness on the electronic structures of $La_3Ni_2O_7$ thin films, arXiv: 2502.04255 (2025)
45. Z. Luo, X. Hu, M. Wang, W. Wu, and D. X. Yao, Bilayer two-orbital model of $La_3Ni_2O_7$ under pressure, *Phys. Rev. Lett.* 131(12), 126001 (2023)
46. G. Li, C. Q. Chen, H. Shi, Z. Liu, H. Ma, F. Tian, D. X. Yao, and D. Duan, Theoretical study on the electronic properties and multiorbital models of $La_3Ni_2O_7$ thin films on $SrLaAlO_4$ (001), arXiv: 2512.17625 (2025)
47. Y. Zhong, W. Wu, and D. X. Yao, Superexchanges and charge transfer in the $La_3Ni_2O_7$ thin films, *Chin. Phys. Lett.* 43(3), 030713 (2026)
48. Y. B. Liu, J. W. Mei, F. Ye, W. Q. Chen, and F. Yang, The $s^{\pm}$-wave pairing and the destructive role of apical-oxygen deficiencies in $La_3Ni_2O_7$ under pressure, *Phys. Rev. Lett.* 131(23), 131 (2023)
49. Y. Zhang, L. F. Lin, A. Moreo, T. A. Maier, and E. Dagotto, Structural phase transition, $s^{\pm}$-wave pairing, and magnetic stripe order in bilayered superconductor $La_3Ni_2O_7$ under pressure, *Nat. Commun.* 15(1), 2470 (2024)
50. Q. G. Yang, D. Wang, and Q. H. Wang, Possible $s^{\pm}$-wave superconductivity in $La_3Ni_2O_7$, *Phys. Rev. B* 108(14), L140505 (2023)
51. K. Y. Jiang, Y. H. Cao, Q. G. Yang, H. Y. Lu, and Q. H. Wang, Theory of pressure dependence of superconductivity in bilayer nickelate $La_3Ni_2O_7$, *Phys. Rev. Lett.* 134(7), 076001 (2025)
52. H. Watanabe, H. Sakakibara, and K. Kuroki, Hierarchical structure of primary and hybridization-induced superconducting correlations in bilayer nickelates, arXiv: 2603.13604 (2026)
53. Y. H. Cao, K. Y. Jiang, H. Y. Lu, D. Wang, and Q. H. Wang, Strain-engineered electronic structure and superconductivity in $La_3Ni_2O_7$ thin films, *Sci. China Phys. Mech. Astron.* 69(4), 247412 (2026)
54. Y. Zhang, L. F. Lin, A. Moreo, S. Okamoto, T. A. Maier, and E. Dagotto, Compressive strain turns $s^{\pm}$ into d-wave pairing in one-unit-cell $La_3Ni_2O_7$ thin film via substrate-induced hole doping, arXiv: 2512.19520 (2025)
55. C. Xia, H. Liu, S. Zhou, and H. Chen, Sensitive dependence of pairing symmetry on Ni-e_g crystal field splitting in the nickelate superconductor $La_3Ni_2O_7$, *Nat. Commun.* 16(1), 1054 (2025)
56. Z. Fan, J. F. Zhang, B. Zhan, D. Lv, X. Y. Jiang, B. Normand, and T. Xiang, B. Normand, and T. Xiang, Superconductivity in nickelate and cuprate superconductors with strong bilayer coupling, *Phys. Rev. B* 110(2), 024514 (2024)
57. Z. Y. Cao, D. Peng, S. Choi, F. Lan, L. Yu, E. Zhang, Z. Xing, Y. Liu, F. Zhang, T. Luo, L. Chen, V. T. A. Hong, S. Y. Paek, H. Jang, J. Xie, H. Liu, H. Lou, Z. Zeng, Y. Ding, J. Zhao, C. Liu, T. Park, Q. Zeng, and H. K. Mao, Direct observation of d-wave superconducting gap symmetry in pressurized $La_3Ni_2O_{7-\delta}$ single crystals, arXiv: 2509.12606 (2025)
58. Z. Luo, B. Lv, M. Wang, W. Wu, and D. -X. Yao, High-T_c superconductivity in $La_3Ni_2O_7$ based on the bilayer two-orbital t–J model, *npj Quantum Mater.* 9, 61 (2024)
59. F. C. Zhang, C. Gros, T. M. Rice, and H. Shiba, A renormalised Hamiltonian approach to a resonant valence bond wavefunction, *Supercond. Sci. Technol.* 1(1), 36 (1988)
60. Q. Qin and Y. F. Yang, Intrinsic constraint on T_c for unconventional superconductivity, *npj Quantum Mater.* 10, 13 (2025)
61. W. Wang, Z. Ma, and H. Q. Lin, A universal scaling law for T_c in unconventional superconductors, arXiv: 2510.25082 (2025)